Wavelength separation from extreme ultraviolet mirrors using phaseshift reflection

A. J. R. van den Boogaard,[1,*] F. A. van Goor,[2] E. Louis,[1] and F. Bijkerk[1,2]
[1]FOM Institute for Plasma Physics Rijnhuizen, P.O. Box 1207, NL-3430BE, Nieuwegein, The Netherlands
[2]MESA+ Institute for Nanotechnology, University of Twente, P.O. Box 217, NL-7500AE, Enschede, The Netherlands
*Corresponding author: a.j.r.vandenboogaard@rijnhuizen.nl

Received November 2, 2011; revised November 18, 2011; accepted November 18, 2011;
posted November 21, 2011 (Doc. ID 157546); published January 10, 2012

A generic design and fabrication scheme of Mo/Si multilayer-grating phaseshift reflector systems is reported. Close to optimized extreme ultraviolet (EUV, $\lambda = 13.5$ nm) reflectance values up to 64% are demonstrated, while the diffractive properties can be exploited in spectral filtering applications. The results can contribute to a wavelength-unspecific solution for the suppression of $\lambda > 100$ nm out-of-band radiation in EUV lithography. © 2012 Optical Society of America

OCIS codes: 230.4170, 230.7408, 340.7480, 050.5080, 050.6875.

Optical multilayers are used as high reflective elements in extreme ultraviolet (EUV, $\lambda = 13.5$ nm) down to the soft x-ray wavelength range. Typically consisting of nanoscale bilayers of a spacer and metal reflector, these structures serve as Bragg-reflecting artificial crystals. For longer wavelengths ($\lambda > 100$ nm) the optical response is similar to efficient single layer mirrors due to the metal fraction in the multilayer. In some applications however, most notably new optical lithography techniques operating at EUV wavelengths [1], optical throughput outside the EUV transmission band is undesirable and the broadband emission properties of the EUV light source imply the necessity of spectral filtering. The out-of-band wavelength ranges concern vacuum ultraviolet (VUV, 100–400 nm) and infrared (IR, mainly 10.6 μm CO_2-laser output), as both present in the spectrum of laser produced Sn-plasma EUV sources [2,3]. Depending on the source spectrum, a 10^{-2} suppression is generally aimed for. Foil or grid transmission filters have been suggested [3], but these cause EUV throughput losses and the fragile filters may not withstand high energy loads.

An increasing amount of attention is attributed to multilayer optics having a more selective spectral response. These could be cooled straightforwardly and ideally could replace a standard multilayer optical element. Multilayers with antireflective layers [4,5,6], as well as multilayer-grating based solutions have been proposed [7,8]. For the latter the filtering principle is based on diffraction caused by the 3D shape of the device, which allows for the use of a thermally stable EUV optimized multilayer, based on alternating Mo/Si layers and optional interface barriers, giving a near-normal peak reflectance up to 70%. The conventional deposition of multilayers on gratings has been demonstrated feasible in applications were spectral resolution is critical [9]. However, the yet obtained device quality in terms of roughness, profile of the facets and multilayer deformations near step-edges still compromises ultimate EUV throughput.

In this Letter an alternative design and unconventional deposition scheme of a multilayer-grating system suited for spectral filtering is reported, with a process flexibility enabling much tighter specifications on multilayer profile and interface quality and hence EUV performance. The system consists of a rectangular multilayer add-structure on a planar substrate-multilayer with a pitch Λ and a step height h. Depending on the application a spacing layer of thickness h_s can be used to reach the desired step height [Fig. 1(a)].

The coverage fraction of the substrate-multilayer by the add-multilayer is chosen 0.5. For near-normal plane-wave illumination conditions this gives equal contributions to the reflected wave front from both regions, whereas a phaseshift is caused by the optical path length difference. Rigorous calculations using the PCGrate software package, reveal that the thus described phaseshift reflector (PsR) will suppress the $m = 0$ order in diffraction for $\lambda = 4h$, yielding a π-phaseshift, hereby diffracting the energy into higher orders of which $m = \pm 1$ have the highest efficiency [Fig. 1(b)]. The suppressed wavelength

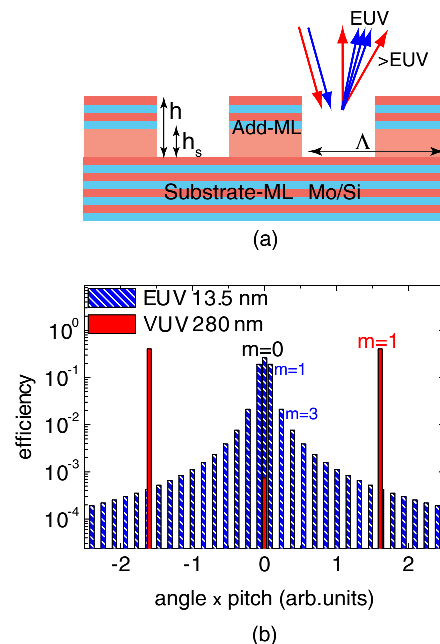

Fig. 1. (Color online) (a) Schematic phaseshift reflector structure. (b) Efficiency orders of diffraction versus angular position for $h = 70$ nm and normal incidence illumination.

0146-9592/12/020160-03$15.00/0 © 2012 Optical Society of America

is scalable and virtually equivalent for VUV and IR; calculated zeroth-order efficiencies of are $\approx 10^{-3}$ in both wavelength ranges. In the EUV the zeroth-order is the most efficient, given that the add-multilayer structure and the substrate-multilayer are in-phase. The near zeroth-orders will typically fall within the angular transmission band of lithographic equipment and closely approach flat multilayer reflectance efficiency; the cumulative efficiency of orders $m \geq |\pm 5|$ is 2%. Since the angular interorder separation is proportional to λ/Λ, as is obtained from the grating equation for near-normal incidence illumination and $\Lambda \gg \lambda$, the described device is suited to spatially separate EUV radiation from longer wavelengths. The PsR is intended to be applied at the EUV source optics in lithography equipment, since there the tolerances to the diffractive response in the EUV are highest. Furthermore, IR transmission is preferably suppressed early in the optical train, to limit the heat load on successive optics.

For demonstration, devices for suppression of VUV (PsR-VUV, $\lambda = 280$ nm) and IR (PsR-IR, $\lambda = 10.6$ μm) have been produced. The deposition scheme was based on the application of a removable contact mask during the deposition of the add-multilayer and optional spacer layer. The substrate-multilayer was deposited in advance onto a substrate of choice and consists of 50 bilayers Mo/Si with a bilayer thickness of 6.95 nm, and a Mo fraction of 0.4. For the PsR-VUV, the add-multilayer consists of 10 bilayers of the same composition as the substrate-multilayer resulting in $h = 69.5$ nm, with no spacer layer ($h_s = 0$). Micromesh foils which are generally utilized as microscopy calibration grids were selected as contact masks. The foils feature a 2D rectangular mesh pattern with square apertures of 18 μm, a wire size of 7.4 μm ($\Lambda = 25.4$), 50% open area, and a thickness of 2–5 μm. The mask thickness/aperture ratio, here denoted as R_a, is an important parameter in the deposition and for the micromesh foils $R_a = 0.1$ to 0.3. This indicates the necessity of a highly isotropic, near-normal deposition flux to obtain sharp replication of the mesh into the deposited structure. Electron beam generated physical vapor deposition (PVD) at high vacuum conditions was employed where the angular spread in incident directions at the sample was in the order of 1° from normal. The demands on deposition angle and isotropy obstruct the use of typically applied off-normal ion-enhanced deposition conditions for smoothest layer growth during the add-multilayer deposition [10]. For the here reported prototypical demonstration, ion assistance was omitted. Furthermore, for the shallow add-multilayer structures agglomeration of roughness is considered to be not critical. The phase requirement of the add-multilayer structure was satisfied by using *in-situ* reflectometry for layer thickness control during deposition. Operating at the C-K$_\alpha$ emission line at 4.47 nm wavelength, the layer thickness control signal was determined by reflections from the layer growth front and several buried interfaces. This enables close matching of the phase of the add-structure with the substrate-multilayer.

For the PsR-IR the add-structure consists of a Si spacer layer $h_s = 2.3$ μm and a 50 bilayer Mo/Si multilayer. The relatively large layer thickness showed to be a complicating factor for two reasons; a thicker foil contact mask had to be applied to prevent mask deformation and displacements caused by layer stresses and electron beam PVD without ion assistance could not be used due to accumulating surface roughness. Instead, magnetron sputter deposition was employed, yielding smooth layers growth as caused by the relatively high energy of the add-atoms (~1 eV against ~0.1 eV for ebeam PVD) and the additional exposure to backscattered target sputtering ions of 10–100 eV. The deposition geometry implies local angle of incidence variations at the sample up to 10°, where the isotropy may be further influenced by the limited mean free path of $\approx 10^{-1}$ m at a working pressure of $\approx 10^{-5}$ mbar. Etched stainless steel line masks with 50% open area and 50 μm thickness were applied. The deposition anisotropy and mask thickness dictated a low mask thickness/aperture ratio and thus large pitch size; $\Lambda = 2$ nm was selected giving $R_a = 0.025$. As an alternative approach, a sacrificial photoresist structure can serve as a contact mask which is removed after deposition of the add-structure in a so-called "lift off" procedure. This currently investigated technique might be beneficial for producing smaller pitches. At a resist thickness (i.e. mask thickness) of 2–3 μm, the requirement of $R_a = 0.025$ would allow for downscaling to pitches of 100 μm. Etching in a multilayer, making use of embedded etch-stop layers, could also be considered [11].

The samples were characterized on EUV reflectance at 1.5° normal angle and with a detector aperture of ±0.5°. EUV reflectance up to 64% is observed for the PsR-VUV sample [Fig. 2(a)], where a reference substrate-multilayer and reference unmasked add-multilayer yield peak reflectance values of 68% and 61%, respectively. The 7% decrease is likely the result of a reduced interface quality in the absence of ion-enhanced growth conditions during the add-multilayer deposition. The wavelength dependency of the PsR-VUV reflectance closely approaches the combined average reflectance of the two reference samples [Fig. 2(a), solid line], advocating a negligible influence of structural deformations near the edges of the add-multilayer, as is in line with reference [12]. Although the data indicate not yet fully optimized reflectance values for none of the two reference systems, an absolute near zeroth-order efficiency of 64% in the EUV wavelength range is the highest reported up till now for any type of reflective wavelength separator, to the best knowledge of the authors. For the PsR-IR, an EUV peak reflectance of 63% has been observed as depicted in Fig. 2(b). This is below the combined average of substrate-multilayer and unmasked add-multilayer [Fig. 2(b), solid line], having a

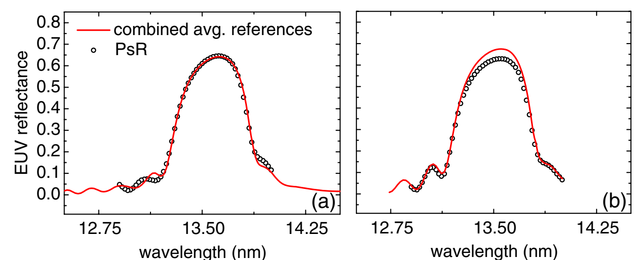

Fig. 2. (Color online) EUV reflectance data (circles) and combined average reference reflectance for (a) PsR-VUV and (b) PsR-IR.

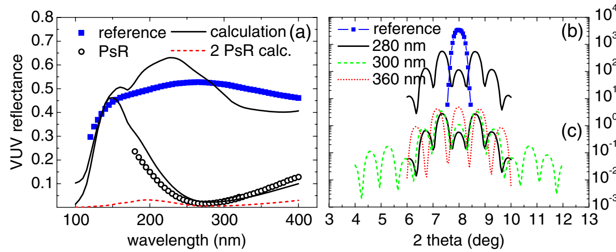

Fig. 3. (Color online) (a) VUV reflectance measurements of a phaseshift reflector (circles) and a reference unstructured multilayer mirror (squares) and calculations (solid lines). Also shown is a calculation of a combined PsR system response (dashed line). (b) Two-theta detector scans at 280 nm for the PsR and reference mirror, offset applied for visualization. (c) Two-theta detector scans PsR at various VUV wavelengths.

peak reflectance of 68% and 67%, respectively. The influence of structural imperfections, i.e. nonflat facets, are probably causing the reflectance decrements. These effects are considered to arise from the anisotropy of the deposition flux, leading to half-shadow regions during the deposition of the add-multilayer near the edges of the mask. Yet, the EUV throughput by the PsR-IR is demonstrated to be well above the theoretic potential of multilayers with antireflection layers.

The diffractive response of the PsR-VUV was measured at the wavelength range of 100–400 nm, an angle of incidence of 4° from normal and an angular resolution <0.4°. Suppression of the zeroth-order with a factor 30 is observed in a broad band around the target wavelength of 280 nm [Fig. 3(a)]. The data is in agreement with rigorous calculations of the zeroth-order in diffraction, accounting for an uncertainty in the pitch of ± 2.5 μm. The bandwidth of the suppression can be further extended, i.e. including the resonant wavelength at $\lambda = 2h$, by a series of phaseshift reflectors optimized for different wavelengths. For two successive systems, one with $\lambda_1 = 4h_1 = 280$ nm and one with $\lambda_2 = 4h_2 = 0.5\lambda_1$, VUV throughput shows a maximum ≤0.03 for the wavelength range 100–400 nm [Fig. 3(a) dashed line]. Detector scans on the intensity profiles of the diffracted VUV radiation at a fixed 4° normal angle of incidence are depicted in Fig. 3(b) and Fig. 3(c). Two-theta defines the angle between the incoming and the diffracted beam. Both the scanning axis and the rectangular PsR-VUV structure were aligned with the incident beam. The zeroth-order suppression with respect to a reference mirror can be observed in Fig. 3(b) and at several VUV wavelengths well separated and symmetric orders in diffraction are shown [Fig. 3(c)], with an angular separation between the first maxima and the zeroth-order of 0.6° at 280 nm wavelength. By the PsR-IR a similar diffractive response as observed in the VUV is considered realizable at $\lambda = 10.6$ μm. The expected interorder separation is 0.3° for $\Lambda = 2$ mm, and 6° for $\Lambda = 100$ μm, as is derived from the grating equation.

In summary, it is demonstrated that deposited multilayer phaseshift reflector structures can serve as a high reflectance optical element in the EUV range (up to 64% reflectance measured) with drastically reduced throughput at out-of-band wavelengths, where a factor 30 reduction has been demonstrated experimentally at 280 nm. As a further advantage, the deposition scheme based on application of a removable contact mask during physical layer deposition, imposes no demands on multilayer composition or substrate material and hence can be considered generically applicable. Sharper mask projections into the deposited add-multilayer structures and application of ion-enhanced layer deposition, will likely enable further optimization of EUV reflectance values. The parameters of main importance are the geometry of the (ion-enhanced) deposition conditions relative to the mask orientation and the contact mask dimensions.

We acknowledge financial support from the AgentschapNL through the EXEPT and ACHieVE programs coordinated by ASML and FOM and Carl Zeiss SMT GmbH through the Industrial Partnership Program XMO.

References

1. V. Banine and R. Moors, J. Phys. D **37**, 3207 (2004).
2. I. V. Fomenkov, D. C. Brandt, A. N. Bykanov, A. I. Ershov, W. N. Partlo, D. W. Myers, N. R. Böwering, G. O. Vaschenko, O. V. Khodykin, J. R. Hoffman, E. Vargas, R. D. Simmons, J. A. Chavez, and C. P. Chrobak, Proc. SPIE **6517**, 65173J (2007).
3. W. A. Soer, M. J. J. Jak, A. M. Yakunin, M. M. J. W. van Herpen, and V. Y. Banine, Proc. SPIE **7271**, 72712Y (2009).
4. M. M. J. W. van Herpen, R. W. E. van de Kruijs, D. J. W. Klunder, E. Louis, A. E. Yakshin, S. Alonso van der Westen, F. Bijkerk, and V. Banine, Opt. Lett. **33**, 560 (2008).
5. W. A. Soer, P. Gawlitza, M. M. J. W. van Herpen, M. J. J. Jak, S. Braun, P. Muys, and V. Y. Banine, Opt. Lett. **34**, 3680 (2009).
6. V. V. Medvedev, A. E. Yakshin, R. W. E. van de Kruijs, V. M. Krivtsun, A. M. Yakunin, K. N. Koshelev, and F. Bijkerk, Opt. Lett. **36**, 3344 (2011).
7. J. A. Liddle, F. Salmassi, P. P. Naulleau, and E. M. Gullikson, J. Vac. Sci. Technol. B **21**, 2980 (2003).
8. A. J. R. van den Boogaard, E. Louis, F. A. van Goor, and F. Bijkerk, Proc. SPIE **7271**, 72713B (2009).
9. D. L. Voronov, M. Ahn, E. H. Anderson, R. Cambie, C.-H. Chang, E. M. Gullikson, R. K. Heilmann, F. Salmassi, M. L. Schattenburg, T. Warwick, V. V. Yashchuk, L. Zipp, and H. A. Padmore, Opt. Lett. **35**, 2615 (2010).
10. A. J. R. van den Boogaard, E. Louis, E. Zoethout, S. Müllender, and F. Bijkerk, J. Vac. Sci. Technol. A **28**, 552 (2010).
11. F. Salmassi, E. M. Gullikson, E. H. Anderson, and P. P. Naulleau, J. Vac. Sci. Technol. B **25**, 2055 (2007).
12. A. J. R. van den Boogaard, E. Louis, E. Zoethout, K. A. Goldberg, and F. Bijkerk, J. Vac. Sci. Technol. B **29**, 051803 (2011).